# Architecture of P2Y Nucleotide Receptors: Structural Comparison Based on Sequence Analysis, Mutagenesis, and Homology Modeling†

Stefano Costanzi, Liaman Mamedova, Zhan-Guo Gao, and Kenneth A. Jacobson*

*Molecular Recognition Section, Laboratory of Bioorganic Chemistry, National Institute of Diabetes and Digestive and Kidney Diseases, National Institutes of Health, Bethesda, Maryland 20892-0810*

*Received January 30, 2004*

Human P2Y receptors encompass at least eight subtypes of Class A G protein-coupled receptors (GPCRs), responding to adenine and/or uracil nucleotides. Using a BLAST search against the *Homo sapiens* subset of the SWISS−PROT and TrEMBL databases, we identified 68 proteins showing high similarity to P2Y receptors. To address the problem of low sequence identity between rhodopsin and the P2Y receptors, we performed a multiple-sequence alignment of the retrieved proteins and the template bovine rhodopsin, combining manual identification of the transmembrane domains (TMs) with automatic techniques. The resulting phylogenetic tree delineated two distinct subgroups of P2Y receptors: $G_q$-coupled subtypes (e.g., $P2Y_1$) and those coupled to $G_i$ (e.g., $P2Y_{12}$). On the basis of sequence comparison we mutated three Tyr residues of the putative $P2Y_1$ binding pocket to Ala and Phe and characterized pharmacologically the mutant receptors expressed in COS-7 cells. The mutation of Y306 (7.35, site of a cationic residue in $P2Y_{12}$) or Y203 in the second extracellular loop selectively decreased the affinity of the agonist 2-MeSADP, and the Y306F mutation also reduced antagonist (MRS2179) affinity by 5-fold. The Y273A (6.48) mutation precluded the receptor activation without a major effect on the ligand-binding affinities, but the Y273F mutant receptor still activated G proteins with full agonist affinity. Thus, we have identified new recognition elements to further define the $P2Y_1$ binding site and related these to other P2Y receptor subtypes. Following sequence-based secondary-structure prediction, we constructed complete models of all the human P2Y receptors by homology to rhodopsin. Ligand docking on $P2Y_1$ and $P2Y_{12}$ receptor models was guided by mutagenesis results, to identify the residues implicated in the binding process. Different sets of cationic residues in the two subgroups appeared to coordinate phosphate-bearing ligands. Within the $P2Y_1$ subgroup these residues are R3.29, K/R6.55, and R7.39. Within the $P2Y_{12}$ subgroup, the only residue in common with $P2Y_1$ is R6.55, and the role of R3.29 in TM3 seems to be fulfilled by a Lys residue in EL2, whereas the R7.39 in TM7 seems to be substituted by K7.35. Thus, we have identified common and distinguishing features of P2Y receptor structure and have proposed modes of ligand binding for the two representative subtypes that already have well-developed ligands.

## Introduction

Human P2Y receptors are a family of nucleotide-activated G protein-coupled receptors (GPCRs), which comprises at least eight distinct subtypes with varying selectivity for adenine or uracil nucleotides and for 5′-diphosphates or 5′-triphosphates.[1] $P2Y_1$, $P2Y_{12}$, and $P2Y_{13}$ receptors are selective for adenine nucleotides, and $P2Y_4$, $P2Y_6$, and $P2Y_{14}$ receptors are selective for uracil nucleotides. The $P2Y_2$ receptor and, according to some evidence, the $P2Y_{11}$ receptor[4] are rather unselective between uracil and adenine nucleotides. Atypical agonist selectivity has been reported for the most recently identified P2Y receptor, the $P2Y_{14}$ receptor,[2,3] which is stimulated by UDP-glucose.

From the perspective of signal transduction, $P2Y_1$, $P2Y_2$, $P2Y_4$, $P2Y_6$, and $P2Y_{11}$ receptors couple preferrentially to the stimulation of phospholipase C (PLC) via $G_q$, and $P2Y_{12}$, $P2Y_{13}$, and $P2Y_{14}$ receptors couple to the inhibition of adenylyl cyclase via $G_i$ (the coupling of $P2Y_{14}$ to $G_i$ has been demonstrated, although the transduction pathways of this receptor in native systems still remain to be defined[3]). The $P2Y_{11}$ receptor was also shown to couple to the stimulation of adenylate cyclase via $G_s$.

The only available template for constructing homology models of GPCRs is the crystal structure of the ground state of bovine rhodopsin,[5] published initially in 2000 by Palczewski and co-workers.[5a] In the present study we carried out a structural comparison of P2Y receptors based on sequence analysis, new and previously reported (Table 1) mutagenesis results, and rhodopsin-based homology modeling. To address the problem of the relatively low sequence identity between rhodopsin and the P2Y receptors (between 15% and 20%), rather than using an automatic pairwise alignment, we performed a combined manual and automatic multiple-sequence alignment. Sequences included in this alignment were bovine rhodopsin, human P2Y receptors, and the sequences contained in the *Homo sapiens* subset of the SWISS−PROT and TrEMBL databases showing a high degree of similarity with P2Y receptors. A phylo-

† Dedicated in honor of Prof. Geoffrey Burnstock on his 75th birthday.

* Correspondence to: Kenneth A. Jacobson, Molecular Recognition Section, LBC, NIDDK, NIH, Bldg. 8A, Rm. B1A-19, Bethesda, MD 20892-0810. E-mail: kajacobs@helix.nih.gov.

10.1021/jm049914c 
Published on Web 09/14/2004

**Table 1.** Inositol Phosphate Accumulation Induced by the Activation of Wild-type and Mutant Human $P2Y_1$ Receptors Transiently Expressed in COS-7 Cells[6,23]

| mutated residue | position | $EC_{50}$ (nM) of 2-MeSADP |
|---|---|---|
| Wild-type | | 1.27 ± 0.01[a] |
| R128A | 3.29 | >100000 |
| F131A | 3.32 | 18.2 ± 2.1 |
| H132A | 3.33 | 15.9 ± 4.4 |
| Y136A | 3.37 | 12.6 ± 1.8 |
| T221A | 5.42 | 15.9 ± 4.0 |
| T222A | 5.43 | 11.2 ± 0.6 |
| F226A | 5.47 | 20.7 ± 3.8 |
| H277A | 6.52 | 100 ± 30 |
| K280A | 6.55 | 1790 ± 310 |
| Q307A | 7.36 | 455 ± 140 |
| R310A | 7.39 | >100000 |
| R310K | 7.39 | 418 ± 118 |
| S314A | 7.43 | >100000 |
| S314T | 7.43 | 11.7 ± 1.8 |
| S317A | 7.46 | 1.58 ± 0.29 |
| C124A | EL1 | >100000 |
| K125A | EL1 | 5.9 ± 7.8 |
| R195A | EL2 | 4.7 ± 0.6 |
| K196A | EL2 | 2.5 ± 0.8 |
| K198A | EL2 | 17.5 ± 2.1 |
| C202A | EL2 | >100000 |
| D204A | EL2 | 66.5 ± 11.5 |
| D204N | EL2 | 595 ± 5.0 |
| D204E | EL2 | 145 ± 15.4 |
| D208A | EL2 | 3.6 ± 0.7 |
| E209A | EL2 | 17200 ± 7400 |
| E209D | EL2 | 3.2 ± 0.6 |
| E209Q | EL2 | 8.6 ± 2.1 |
| E209R | EL2 | 4.9 ± 1.3 |
| R212A | EL2 | 7.8 ± 5.5 |
| R285A | EL3 | 9.2 ± 5.4 |
| R287A | EL3 | 14800 ± 2600 |
| R287K | EL3 | 74.9 ± 5.5 |
| R287Q | EL3 | 5290 ± 360 |
| R287E | EL3 | >100000 |
| D289A | EL3 | 3.9 ± 0.4 |
| C296A | EL3 | 5160 ± 920 |
| D300A | EL3 | 9.8 ± 0.5 |
| R301A | EL3 | 2.6 ± 0.3 |

[a] In a separate experiment the potency of 2-MeSADP at the wild-type human $P2Y_1$ receptors was 2.2 ± 0.5 nM.[6]

genetic analysis was also carried out to establish the relationships among the various subtypes of P2Y receptors and finding their similarity with other known and orphan GPCRs. On the basis of the bioinformatic analysis and previous molecular modeling,[6−9] we mutated three Tyr residues located in the putative $P2Y_1$ binding pocket to Ala and Phe and studied the pharmacological properties of the mutated receptors in stimulation and ligand binding. We applied the results of mutagenesis and sequence alignment to construct complete homology models[10,11] of all human P2Y receptor subtypes. On these models we performed docking experiments, guided by mutagenesis results, at two P2Y subtypes for which potent antagonist ligands (**1**−**3**, Chart 1) are known. The docking experiments serve to identify amino acid residues likely to be involved in the binding process and to generate information on the topology of the binding site.

## Results and Discussion

**Sequence Analysis of P2Y Receptors in Relation to Similar GPCRs.** We performed a BLAST search against the *H. sapiens* subset of the SWISS−PROT and TrEMBL databases with $P2Y_1$ and $P2Y_{12}$ receptors as probes. After the elimination of the isoforms of proteins already present in the list, we obtained a nonredundant set of amino acid sequences of 68 GPCRs, including eight P2Y receptors and sequences showing a high degree of similarity with P2Y receptors.

**Chart 1.** Agonists and Antagonists at $P2Y_1$ and $P2Y_{12}$ Receptors Used in Docking and Binding Studies

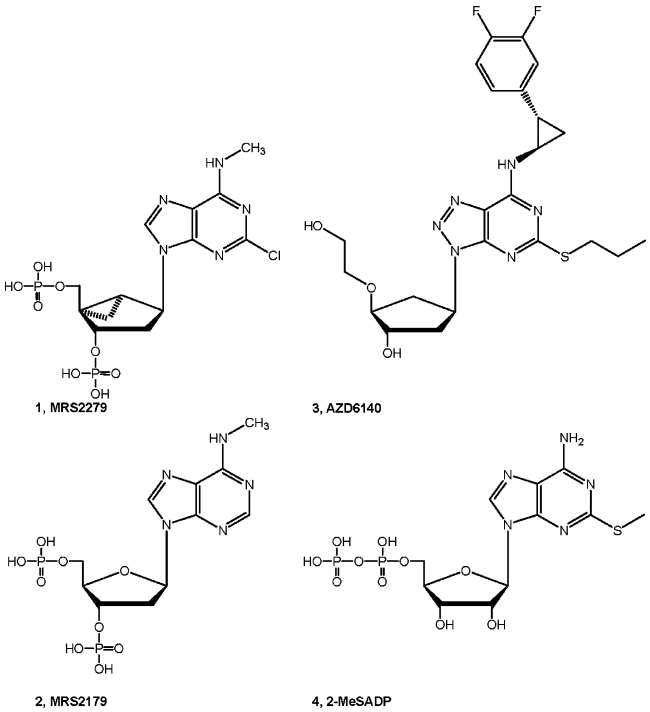


**Multiple Sequence Alignment.** A multiple sequence alignment of all the proteins belonging to this family was completed, combining the manual alignment of the TMs with automatic multiple sequence alignment techniques for the loop regions, according to the protocol described in Materials and Methods. The presence of a large number of sequences minimized the errors arising from the very low sequence identity present in the loop regions.

The alignment included the sequence of bovine rhodopsin, which is the only GPCR whose three-dimensional structure has been experimentally disclosed.[5] This allowed us to take into consideration the three-dimensional information obtained from the secondary and tertiary structure of the template, to avoid the introduction of gaps or amino acid insertions in positions incompatible with the structure of the template. The resulting manual/automatic alignment was manually refined iteratively with the construction of the homology models (see the Homology modeling paragraph for more detail).

The alignment of P2Y receptor subtypes and bovine rhodopsin is reported in Figure 1, and the complete alignment of all the sequences is presented in Clustal[12,13] format as Supporting Information.

**Phylogenetic Analysis.** By using the Neighbor-Joining method[14] on a distance matrix obtained by applying the PAM amino acid substitution model[15] to our sequence alignment, we constructed a phylogenetic tree that reflected the relationships between the various subtypes of P2Y receptors and the other proteins that were retrieved with the BLAST search (Figure 2).

The tree was clearly divided into two main branches. The first branch (upper right side in Figure 2) showed

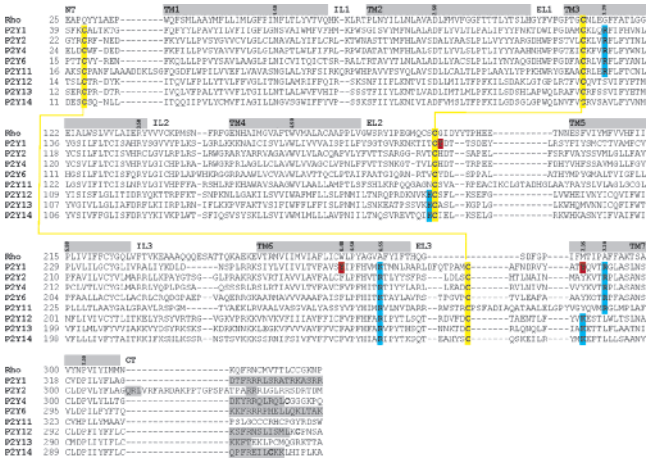

**Figure 1.** Sequence alignment of bovine rhodopsin and human P2Y receptors. The TMs, as deduced from the bovine rhodopsin X-ray crystallographic structure are highlighted, and the amino acid identifiers for the most conserved residues of each TM are shown. The basic amino acids involved in phosphate coordination are highlighted in cyan and their amino acid identifiers indicated; the amino acids mutated in this work are highlighted in red; the Cys residues involved in putative disulfide bridge formation in P2Y receptors, based on sequence comparison, are highlighted in yellow and connected by a yellow line to represent the bridge. The residues predicted to assume an α-helical conformation in the cytoplasmatic extension of TM7, known as H8, are highlighted in green (secondary-structure prediction based on MLRC method). By homology with bovine rhodopsin, it can be proposed that Cys residues (here represented in bold) facing the cell membrane present in proximity to the carboxyl-terminal end of H8 in $P2Y_4$, $PY_{12}$, and $P2Y_{14}$ might be palmitoylated to provide an anchor of H8 to the membrane.

the presence of two phylogenetically distinct subgroups of P2Y receptors, one encompassing the receptors that mainly couple to the $G_q$ protein, and the other containing receptors that couple to the $G_i$ protein. The first subgroup was comprised of $P2Y_1$, $P2Y_2$, $P2Y_4$, $P2Y_6$, and $P2Y_{11}$ receptors. The average pair distance between these proteins, which was calculated according to the PAM method and expressed in units of expected fraction of amino acids changed, was ∼1.17. Less closely related was the $P2Y_{11}$ receptor, which showed an average distance from the other receptors of ∼1.89. The second family comprised $P2Y_{12}$, $P2Y_{13}$, and $P2Y_{14}$ receptors and showed an average pair distance between its members of ∼0.97. The average pair distance between the two families was ∼2.26, with the exception of $P2Y_{11}$, which showed an average distance of ∼2.65 from $P2Y_{12}$, $P2Y_{13}$, and $P2Y_{14}$.

Also, receptors for lipid mediators were present in this branch of the tree, including two different subtypes of cysteinyl leukotriene receptors and a receptor for the phospholipid platelet-activating factor. Sphingosylphosphorylcholine and lysophosphatidylcholine were recently identified as the natural ligands for three receptors known as GPR68 (OGR1), GPR4, and G2A,[16] and P2y9 (GPR23) was identified as a receptor for lysophosphatidic acid. [17]

Three different subtypes of protease-activated receptors (PARs) belonged to this branch. These receptors are activated by the enzyme thrombin (or trypsin in the case of PAR2), which cleaves their amino-terminal exo domain to unmask the amino terminus of an autostimulated receptor. The cleaved peptide serves as a tethered peptide ligand, binding intramolecularly to the body of the receptor.[18]

HM74 was recently identified as a low-affinity receptor for nicotinic acid.[19] Besides P2Y receptors, this is the only receptor within this subfamily of GPCRs that is known to respond to a small-molecule agonist. The other receptors belonging to this branch, including $P2y_5$, $P2y_9$, and $P2y_{10}$, fall in the category of orphan receptors, with their endogenous ligands still unknown.

The other branch of the tree encompasses mainly receptors for peptides. The phylogenetic tree (Figure 2) showed the relatedness of opioid peptide, somatostatin, apelin, angiotensin, and chemokine receptors. The only exceptions were the leukotriene B4 receptors $BLT_1$ and $BLT_2$. $BLT_1$ is also known as $P2y_7$ due to its early erroneous identification as a P2Y subtype. RDC1 is still categorized as an orphan receptor.

The tree was highly dependent on the sequence alignment, the scoring matrix, and the algorithm used. Other recently published works[20,21] reported automatically obtained phylogenetic trees for a great number of GPCRs, giving a broad overview of the superfamily. Our tree covered a smaller (yet significant) region of GPCRs; however, due to the particular technique used for the alignment, the tree was more accurate regarding these particular receptors. The statistical robustness of the Neighbor-Joining tree and reliability of the branching patterns were confirmed by generating 100 bootstrap replications of the sequence alignment. The obtained average consensus tree showed the same relationships between the two subfamilies of P2Y receptors and the other proteins as the original tree, proving that the results of this analysis were not affected by small local changes in the alignment.

**Disulfide Bridges.** Our sequence alignment clearly showed that the Cys residues of the disulfide bridge that linked the amino-terminal region to EL3 of the $P2Y_1$ receptor[6] were conserved among all P2Y subtypes and the great majority of the other GPCRs belonging to this subfamily (Figure 1). The only exceptions were opioid receptors, somatostatin receptors, leukotriene B4 receptors, PARs, PAF receptor, CXCR6 chemokine receptor, and the orphan receptors GPR87 and GPR91. Furthermore, like the vast majority of GPCRs, all of the receptors included in our phylogenetic tree contained the highly conserved Cys residues that, as confirmed by the crystal structure of bovine rhodopsin, are likely to be involved in the formation of a disulfide bridge connecting EL2 with the upper part of TM3.

**Primary and Secondary Structure Analysis of the Carboxyl-Terminal Regions.** We studied the topology of the initial residues of the carboxyl-terminal domain of P2Y receptors in comparison with those of bovine rhodopsin. The crystal structure of bovine rhodopsin[5] confirmed the presence of an α-helical structure in the carboxyl-terminal region, as a cytoplasmatic extension of TM7. This helix, known as H8, lies nearly perpendicular to TM7, to which it is connected by a helix-turn-helix structure containing the D/NPxxY(x)5,6F motif, which is conserved in the majority of Class A GPCRs. According to experimental evidence, a hydrophobic interaction between the two aromatic residues of the D/NPxxY(x)5,6F motif is present

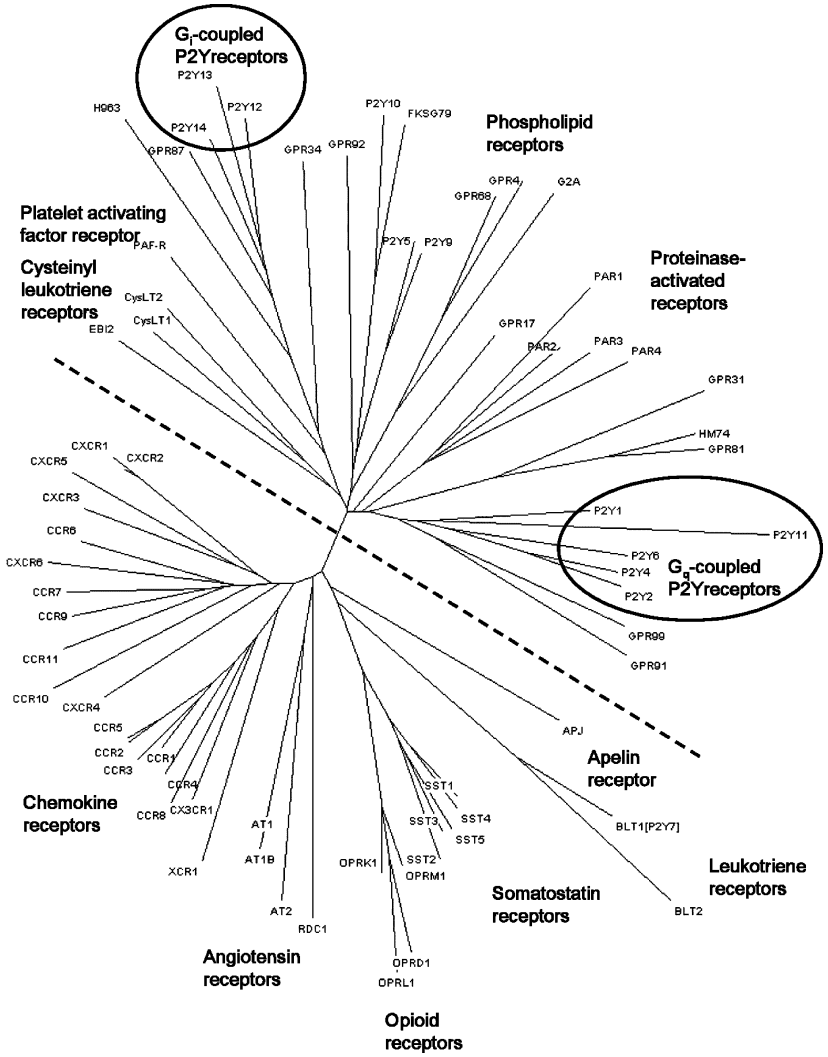


**Figure 2.** Phylogenetic tree obtained by using the Neighbor-Joining method on a distance matrix obtained applying the PAM substitution model to our multiple-sequence alignment. The tree is clearly divided into two main branches, separated by a dashed line. The first branch shows the presence of two phylogenetically distinct subgroups of P2Y receptors, one encompassing the receptors that mainly couple to the $G_q$ protein, and the other containing the receptors that couple to the $G_i$ protein. The other branch of the tree encompasses mainly receptors for peptides.

in the ground-state rhodopsin and should be disrupted during the MetaI/MetaII transition.[5,22] H8, in rhodopsin, ends with two palmitoylated Cys residues (C322 and C323), which anchor this short helix to the membrane.

The P2Y receptors, with the exception of $P2Y_2$ and $P2Y_{11}$, also show the D/NPxxY(x)5,6F motif at the cytoplasmatic end of TM7. Therefore, we studied the tendency of amino acids in these regions to adopt an α-helical organization. For all P2Y receptor subtypes, with the exception of $P2Y_2$ and $P2Y_{11}$, an α-helical structure was predicted for the initial part of the carboxyl-terminal region. The length of this short helix was different for each subtype (Figure 1). As for rhodopsin, in the case of $P2Y_4$, $P2Y_{12}$, and $P2Y_{14}$ receptors, a Cys residue facing the cell membrane was present near the carboxyl-terminal end of H8. It could be argued that these Cys residues, as in the case of rhodopsin, might be palmitoylated to provide an anchor for H8 to the membrane. Thus, in homology modeling we assumed the presence of an α-helical structure of appropriate length, homologous to H8 of rhodopsin, in all P2Y receptors, except for $P2Y_2$ and $P2Y_{11}$. Since we did not find evidence of such an α-helical structure for $P2Y_2$ and $P2Y_{11}$ receptors, we did not model the regions for these two subtypes.

**Site-Directed Mutagenesis of the Human $P2Y_1$ Receptor.** The putative nucleotide-binding site of the human $P2Y_1$ receptor was identified by site-directed mutagenesis experiments,[6,7,23] in which residues from TM3, TM6, TM7, and EL2 were found to be involved in the processes of ligand recognition and/or receptor activation (Table 1). In particular, the residues R128-(3.29), K280(6.55), Q307(7.36), R310(7.39), and S314-(7.43) were found essential for the recognition of nucleotide ligands.[23] Furthermore, mutation of D204(EL2) to Ala, Glu, or Asn impaired the agonist-promoted activation of the receptor.[6]

On the basis of sequence comparisons and previous molecular modeling studies,[6,7,8,9] we further characterized the putative binding region of the $P2Y_1$ receptor by mutating various Tyr residues located in TM6, TM7, and EL2 to Ala and Phe. In particular, the three residues selected for substitution were Y203 in EL2, Y273(6.48) in TM6, and Y306(7.35) in TM7. Y203 was chosen to gain insight into the role of EL2. This residue is located in a crucial position between the C202

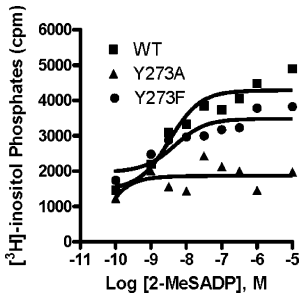


**Figure 3.** Stimulation of PLC by 2-MeSADP in COS-7 cells transiently expressing either WT or mutant human $P2Y_1$ receptors. After labeling with *myo*-[$^3$H]inositol (1 $\mu$Ci/$10^6$ cells) for 24 h, the cells were treated for 30 min at 37 °C with the agonist 2-MeSADP **4**. The amount of inositol phosphates was analyzed after extraction though Dowex AG 1-X8 columns (see Materials and Methods). Data shown are mean values from two to three experiments.

involved in the formation of the putative disulfide bridge with C124(3.25) and the essential D204. Y273(6.48) in TM6 was the residue corresponding to W243(6.48) of the $A_3$ adenosine receptor. The importance of residue 6.48 for the $A_3$ adenosine receptor and for other GPCRs has already been established: it is located in the agonist-binding pocket,[24,25] and according to modeling and mutagenesis data, seems to act as a molecular switch for receptor activation.[25] Y306 was chosen because it is located at a distance of four residues—i.e., one helix turn above—from the key cationic residue R310(7.39).[23] Furthermore, this residue corresponded to a prominent positively charged residue in the $P2Y_{12}$ receptor, K280(7.35), which was later implicated in an ionic interaction with an agonist ligand (see the Docking Studies paragraph for details).

All of the mutant receptors, together with the wild-type (WT) receptor, were tested using a functional assay of PLC (Figure 3, Table 2) and in a radioligand ([$^3$H]**1**) binding assay (Figure 4, Table 2) with 2-MeSADP **4** as agonist and MRS2179 **2** as antagonist (Chart 1). In a direct analogy to the W(6.48)A mutation of the $A_3$ adenosine receptor,[25] the Y273A (6.48) mutation led to a functionally inactive receptor incapable of being stimulated by the agonist. However, this change in the $P2Y_1$ receptor did not have a major effect on the binding affinity of either agonist **4** or antagonist **2**. In contrast, at the $A_3$ adenosine receptor, antagonist affinity was selectively reduced by the W(6.48)A mutation. The Y273F mutant receptor still activated G proteins with agonist potency similar to WT; thus, an aromatic side chain (phenyl ring) sufficed at this position for receptor activation. This suggested that in the case of the $P2Y_1$ receptor, the role of the residue at the 6.48 position in signal transmission was not mediated by the formation or the disruption of hydrogen bonds by its side chain. In all the subtypes of P2Y receptors, with the exception of $P2Y_1$ and $P2Y_{11}$, a Phe residue occurred naturally at position 6.48.

The other mutations modulated to various extents the affinity of the receptor for the agonist and the antagonist, but did not preclude G protein coupling. All of the mutant receptors, including Y273A and Y273F, showed a 1.5 to 4.5-fold reduced affinity for the antagonist MRS2179 **2**. The Y306A and the Y306F mutant receptors showed approximately a 10-fold reduced affinity for the agonist 2-MeSADP **4**. Strikingly, 2-MeSADP **4**, failed to compete for binding of radioligand at the Y203A mutant receptor, while it showed only an 11-fold reduced affinity for the Y203F mutant. Thus, an aromatic residue at this position is required for agonist recognition.

**Homology Modeling of the P2Y Receptor Family.** In the absence of a crystallographic structure of any P2Y receptor, we have used the imprecise method of rhodopsin-based homology modeling of Family 1 GPCRs. Using that approach, overall architecture may be predicted reasonably; however, the details of small molecule recognition are more difficult to predict. The generally accepted assumption is that the overall structure of the helical bundle of the GPCRs is conserved among all the members of the superfamily. We constructed complete homology models of all the subtypes of P2Y receptors with the program Modeler.[26,27]

By means of the loop refinement feature of Modeler,[26,27] we generated five different models for the loop regions of each receptor. For all the subtypes we made use of the two putative disulfide bridges, even though one of them has been proven to be nonessential for the functional $P2Y_{12}$ receptor.[51] These disulfide bridges furnished two external constraints that helped to define the conformation of these very flexible regions. After an evaluation of the resulting models with internal (probability density functions and energy evaluation) and external (Procheck[28]) checks, we identified the loop regions showing high energy values or violations of the stereochemical restraints. Then, we manually modified the sequence alignment and completely reconstructed the models to obtain improved structures. This process was repeated iteratively until no further improvement was possible. Each selected model was then optimized by means of 50-ps molecular dynamics and energy minimization as described in Materials and Methods.

Through this protocol we obtained models for the eight P2Y receptors that resembled the structure of bovine rhodopsin in the helical bundle, in the intracellular H8 (in the cases in which we hypothesized the presence of such a structure), and in EL2, which is the only loop that shows a defined secondary structure in the crystal structure of bovine rhodopsin. The only significant deviations were found in the remaining, flexible intracellular and extracellular regions.

The RMS (root-mean-squared) deviation between the backbone atoms of the seven TMs of P2Y receptors and rhodopsin was always lower than 0.79 Å (Supporting Information). The antiparallel $\beta$-sheet of EL2 characteristic of the crystal structure of the ground state of bovine rhodopsin was detected in all our models of the ground-state P2Y receptors. This loop appeared to be constrained in its position by means of the disulfide bridge that linked it to the upper part of TM3.

The stereochemical quality of the optimized receptor models was checked for all the stereochemical parameters using the program Procheck.[2829] The results were similar to or better than the 2.8-Å crystal structure of the template. In particular, all the residues of the TM were found within the energetically favorable region of the right-handed $\alpha$-helix of the Ramachandran plot. Only a few amino acids (from a minimum of 0.7% in the case of $P2Y_1$ receptors to a maximum of 2.2% in the

**Table 2.** Potency of the Agonist 2-MeSADP **4** and the Antagonist MRS2179 **2** in Binding and Functional Assays at Wild-type and Mutant Human $P2Y_1$ Receptors

| | WT | Y203A (EL2) | Y203F | Y273A (6.48) | Y273F | Y306A (7.35) | Y306F |
|---|---|---|---|---|---|---|---|
| potency of **4**,[a], $EC_{50}$ (nM) | 3 ± 1 | >10000[c] | 16 ±5 | >10000[c] | 6 ± 3 | 15 ±2 | 19 ±7 |
| binding of **4**,[b] $IC_{50}$ (nM) | 24 ± 12 | >10000[d] | 260 ± 80 | 22 ± 1 | 40 ± 20 | 150 ± 40 | 360 ± 150 |
| binding of **2**,[b] $IC_{50}$ (nM) | 210 ± 30 | 740 ± 50 | 330 ± 160 | 480 ± 190 | 660 ± 210 | 320 ± 20 | 980 ± 10 |

[a] Stimulation of PLC by **4** in COS-7 cells transiently expressing either wild type or mutant human $P2Y_1$ receptors. The baseline control value was 1680 ± 200 counts, and 100% stimulation was equal to 5730 ± 580 counts. [b] Displacment of [$^3$H]**1** in membranes of COS-7 cells transiently expressing either wild type or mutant human $P2Y_1$ receptor. [c] No stimulation observed up to 10 $\mu$M of **4**. [d] <10% displacement of binding observed at 10 $\mu$M of **4**.

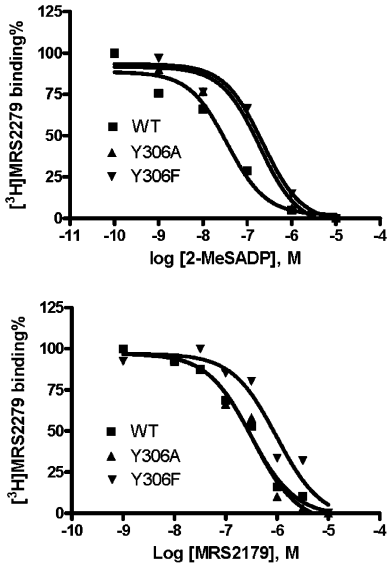


**Figure 4.** Human $P2Y_1$ selective binding of [$^3$H]**1** in membranes prepared from COS-7 cells transiently expressing either WT or mutant human $P2Y_1$ receptors. The membranes prepared from cells (40 $\mu$g protein/tube) were incubated with 8 nM [$^3$H]**1** and (a) varying concentrations of the agonist 2-MeSADP or (b) varying concentrations of the antagonist **2**.

case of $P2Y_4$ and $P2Y_6$ receptors) located at the interface between the loops and the TMs were found in the disallowed region of the Ramachandran plot.

We constructed our models of P2Y receptors to approximate as closely as possible the structure of the ground state (resting or inactive) of bovine rhodopsin. These models provide useful tools to generate hypotheses about the molecular features that stabilize the ground states of the P2Y receptors, to give a rational interpretation to the structure−activity relationship (SAR) data, and to project new targeted site-directed mutagenesis experiments. In future studies these models could be embedded in a phospholipid bilayer[30] to explore, by means of an extensive molecular dynamics simulation, the allowed conformation and to gain insight into the mechanism of activation. The coordinates of all receptor models are given in Supporting Information in PDB format.

**Interhelical H-Bonds: Rhodopsin Compared to P2Y Receptors.** These models, representing the inactive states of the P2Y receptors, appeared to be stabilized by networks of hydrogen bonds connecting TM1 with TM7, TM2 with TM4, and TM3 with TM6 and TM7. Some of these H-bonds were conserved in rhodopsin, and others typified P2Y receptors (Table 3).

Highly conserved among all P2Y receptors were the hydrogen bonds between the amino acids 1.50−7.46 and 4.50−2.45, connecting an Asn residue in TM1 with a backbone carbonyl of TM7 and a conserved Trp in TM4 with a residue capable of accepting an H-bond in TM2, respectively. These two H-bonds are probably conserved among the majority of GPCRs and are present in the 2.8-Å crystal structure of bovine rhodopsin. According to our models, in the majority of P2Y receptor subtypes, the association between TM2 and TM4 is strengthened by an additional H-bond, in which residue 2.45 acts as an acceptor from a Ser or a Cys residue present at position 4.46.

The crystal structure of rhodopsin also reveals an H-bond network spanning the lower parts of TM3 and TM6. The carboxylate of E134 (3.49) of rhodopsin, part of the highly conserved (D/E)R(Y/W) motif in GPCRs, and the guanidine group of R135 (3.50) were linked by a salt bridge. The latter also acted as a H-bond donor to E247 (6.30) and T251 (6.34), connecting TM3 and TM6. These interactions were not conserved in the P2Y receptors, due to the lack of sequence identity. Our models suggested that in the case of the P2Y receptors, the linkage between TM3 and TM6 could be provided by the H-bond that a basic residue, present at position 6.30, could donate to the residue at position 3.49. Furthermore, we detected an additional H-bond between the Arg residue at position 3.50 and a residue capable of accepting an H-bond at position 6.34 present only in the models of the members of the $P2Y_{12}$-like subfamily. In the $P2Y_1$-like subfamily, a hydrophobic residue always occupied position 6.34.

Furthermore, our P2Y receptor models suggested the existence of two additional interhelical H-bonds, present in all or most subtypes, that connected TM7 with TM1 and TM3 through interactions between residues highly conserved in this family but not in rhodopsin. The side chains of S7.43 and N7.45, for example, were always linked with those of Y1.39 and N3.39, respectively. An additional H-bond between the side chain of highly conserved Tyr present at position 7.53 (NPxxY(x)5,6F motif) and the side chain of a hydrophilic residue at position 2.40 was detected in both $P2Y_1$ and $P2Y_2$ subtypes.

**Docking of Potent $P2Y_1$ and $P2Y_{12}$ Receptor Agonists and Antagonists.** Having delineated two subgroups of P2Y receptors by a phylogenetic analysis, we wanted to characterize the putative ligand-binding site of one member of each family to investigate the analogies and differences in the mechanism of ligand recognition. Furthermore, having constructed the homology models of all the subtypes of P2Y receptors, we were able to extend our conclusions to the other subtypes of the two subgroups by means of superimpositions and preliminary docking experiments.

Most current information on mutagenesis of P2Y receptors, both from previous studies[6,7,23] and in the

**Table 3.** Interhelical Hydrogen Bond Networks in the Ground State of the Human P2Y Receptors, as Predicted Using the Homology Models

| | sequence identifier | | | | | | | |
|---|---|---|---|---|---|---|---|---|
| donor−acceptor | $P2Y_1$ | $P2Y_2$ | $P2Y_4$ | $P2Y_6$ | $P2Y_{11}$ | $P2Y_{12}$ | $P2Y_{13}$ | $P2Y_{14}$ |
| 1.50−7.46[a,b] | N69−S317 | N51−S299 | N53−S299 | N44−S294 | N54−F322 | N43−A291 | N41−I289 | N40−V288 |
| 1.39−7.43 | Y58−S314 | Y40−S296 | Y42−S296 | Y33−S291 | *c* | Y32−S288 | *c* | *c* |
| 4.50−2.45[a] | W176−N92 | W158−H74 | W160−H76 | W152−N67 | W162−Q78 | W149−N65 | W147−N63 | W146−N62 |
| 2.45−4.46 | N92−S172 | *c* | H76−C156 | N67−C148 | Q78−S158 | N65−S145 | N63−S143 | N62−S142 |
| 6.30−3.49[a] | R255−H148 | K240−H130 | R240−H132 | R234−Q123 | K251−N134 | R231−D121 | N229−D119 | K228−D118 |
| 3.50−6.34[a] | *c* | *c* | *c* | *c* | *c* | R122−N235 | R120−E233 | R119−S232 |
| 7.45−3.39 | N316−S138 | N298−S120 | N298−S122 | N293−S113 | *c* | N290−S111 | *c* | N287−S108 |
| 7.53−2.40 | Y324−S87 | Y306−T69 | *c* | *c* | *c* | *c* | *c* | *c* |

[a] H-bond conserved in bovine rhodopsin as confirmed by the 2.8 Å crystal structure.[5] [b] Residue 7.46 accepts the hydrogen bond by means of the backbone carbonyl oxygen. All other H-bonds are established between the side chains of the involved amino acids. [c] No H-bond possible between corresponding residues.

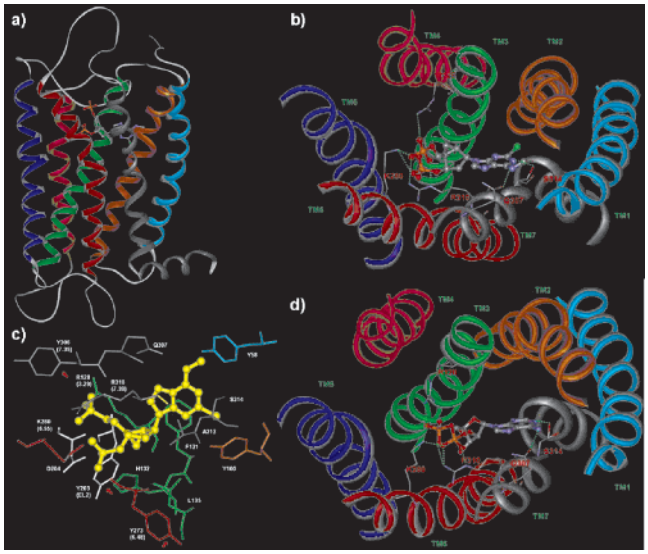


**Figure 5.** Complexes of the $P2Y_1$ receptor with the potent antagonist **1** and with the agonist ADP. Color of TMs: cyan (TM1), orange (TM2), green (TM3), magenta (TM4), blue (TM5), red (TM6), gray (TM7). (a) View from the plane of the cell membrane of $P2Y_1$-**1** complex. (b) View from outside the cell of $P2Y_1$/**1** complex. c) View of the bisphosphate **1** within the binding pocket of $P2Y_1$. For the three key cationic residues and for the three mutated Tyr residues the amino acids identifiers are shown; red arrows indicate the mutated Tyr. d) View from outside the cell of $P2Y_1$-ADP complex.

present work, has been collected for $P2Y_1$ receptors. Furthermore, our homology models were based on the inactive state of rhodopsin. Following these considerations, we adopted a docking strategy to initially study the interactions between the $P2Y_1$ receptor and its potent, conformationally constrained antagonist **1** (Chart 1), previously synthesized by our lab.[31] A second step involved studying the interactions between the $P2Y_1$ receptor and its natural ligand, ADP. Because $P2Y_1$ and $P2Y_{12}$ share the same natural agonist, in the third step we used the information deduced from the $P2Y_1$-ADP complex to dock ADP into the $P2Y_{12}$ receptor. Finally, we studied the interactions between the $P2Y_{12}$ receptor and the nucleoside-like antagonist of nanomolar potency, AZD6140 **3**, developed by Astra-Zeneca for treating arterial thrombosis.[32]

**Docking at $P2Y_1$ Receptors.** The results of the docking studies of the rigid methanocarba antagonist **1** and the flexible agonist ADP at the $P2Y_1$ receptor are shown in Figure 5. The antagonist **1** bound to $P2Y_1$ in the exofacial side of the cavity delineated by TM3, TM6, and TM7 and capped with EL2, with the phosphate groups accommodated in a positively charged pocket formed by R128(3.29), K280(6.55), and R310(7.39). The sequence comparisons showed that the residues R3.29 and R7.39 were conserved among all subtypes of the first subgroup of P2Y receptors; the subtypes belonging to the second subgroup did not show the presence of basic amino acids at these positions. However, a basic residue at position 6.55, which was a Lys in the case of $P2Y_1$ and $P2Y_6$ and an Arg in all other cases, was conserved among all the members of the two subgroups.

Q307(7.36) accepted a hydrogen bond from the amine at the 6-position of the purine ring and was available to donate a hydrogen bond to the nitrogen at the 7-position. The presence of a Gln residue at position 7.36 was typical of the adenine nucleotide-binding P2Y receptors within the first subgroup, $P2Y_1$ and $P2Y_{11}$. The uracil nucleotide-accepting receptors $P2Y_2$, $P2Y_4$, and $P2Y_6$ instead showed the presence of a Lys at position 7.36, which, according to our preliminary docking experiments, could be responsible for the formation of a hydrogen bond with the carbonyl oxygen group at the 4-position of the uracil ring. Site-directed mutagenesis experiments would be necessary to confirm whether this Lys residue plays the fundamental role suggested by the models. The receptors belonging to the second subgroup ($P2Y_{12}$, $P2Y_{13}$, and $P2Y_{14}$) always showed a Glu residue at position 7.36.

S314(7.43) donated a hydrogen bond to the nitrogen at the 1-position of the purine ring. This residue was conserved among all subtypes belonging to the first subgroup of P2Y receptors, except for the $P2Y_{11}$ receptor, in which a Pro residue was present at position 7.43. Ser was also present at position 7.43 in the $P2Y_{12}$ receptor, and an Ala was present in the $P2Y_{13}$ and $P2Y_{14}$ receptors.

Our calculations suggested a binding mode for ADP that is very similar to that of the bisphosphate **1**, in good agreement with the available mutagenesis data.[23] These data emphasized the fundamental role in the recognition of agonists and antagonists played by three basic residues in the $P2Y_1$ receptor at positions 3.29, 6.55, and 7.39, as well as the importance of the presence of Q7.36 and S7.43, The 5′-diphosphophosphate group of ADP was coordinated by R128(3.29), K280(6.55), and R310(7.39), and the purine ring formed the same interactions with Q307(7.36) and S314(7.43).

Consistent with the $P2Y_1$ receptor homology model and ligand docking, the hydroxyl groups of the three Tyr residues mutated in this work did not play a crucial

role in ligand recognition and did not seem to be involved in the formation of inter- or intramolecular hydrogen bonds.

As suggested by the mutagenesis data, Y273(6.48), which plays a fundamental role in the activation of the receptor, was not directly involved in the formation of the binding pocket for either agonist or antagonist. Furthermore, unlike W243(6.48) in the $A_3$ adenosine receptor,[25] the side chain of Y273(6.48) did not appear to be directly implicated in the formation of the hydrogen bond network to stabilize the ground state of the receptor. We could speculate that the importance of Y273(6.48) in the $P2Y_1$ receptor is in transmitting a rotation induced by the binding of the agonist in the upper part of TM6. This might occur through the interaction of a phosphate moiety with K280(6.55), to the lower part of the helix by means of interactions with conserved aromatic amino acids present above and below position 6.48: i.e., F269(6.44), F276(6.51), and H277(6.52). By homology, this hypothesis could be extended to the other P2Y receptors. Supporting this hypothesis, mutation of H277(6.52) in the $P2Y_1$ receptor to Ala resulted in the loss of activation by nucleotide agonist but not in binding of the nucleotide antagonist **2** or a nonnucleotide antagonist (a pyridoxal phosphate derivative), suggesting that this residue may be critical for agonist binding and/or activation processes.[7,23,33] A His residue also appears at the position 6.52 in adenosine receptors and is involved in ligand recognition.[25]

The mutation of Y203(EL2) and Y306(7.35) seemed to have a modulatory effect on the binding of both agonist and antagonist. As expected, these residues appeared from our model to be located in a phosphate-binding pocket and appeared proximal to the crucial cationic residues. In particular Y203(EL2) appeared to play a major role in the recognition of the agonist, and the presence of an aromatic residue was essential at this position. In our model Y203 is located in close proximity to the essential D204(EL2) and K280 (6.55). According to our model, D204(EL2) is engaged in a hydrogen bond with K280 in the ground state of the $P2Y_1$ receptor. It could be speculated that, after the conformational change of the $P2Y_1$ receptor necessary for the binding of the agonist, Y203(EL2) might be engaged in a cation$-\pi$ bond with K280 (6.55).

**Docking at $P2Y_{12}$ Receptors.** As a result of the automatic docking of ADP into the $P2Y_{12}$ receptor, we obtained a complex showing an overall binding mode similar to that of $P2Y_1$ (Figure 6), with the ligand accommodated in the pocket formed by the upper part of TM3, TM6, and TM7 and closed by EL2. Nevertheless, two of the three basic amino acids involved in the coordination of the phosphates were different. R256-(6.55) of $P2Y_{12}$ corresponding to K280(6.55) in the $P2Y_1$ receptor was the only key cationic residue in common between the two subgroups. The importance of this residue was also suggested by a malfunctioning of platelet aggregation in a patient with a naturally occurring R256Q mutation of the $P2Y_{12}$ receptor.[34] The function of R128(3.29) in TM3 as a phosphate counterion appeared to be filled in the second subgroup by a Lys in EL2. The role of R310(7.39) in TM7 in coordinating the phosphate group could be substituted in the second subgroup by K280(7.35), located one helical turn toward

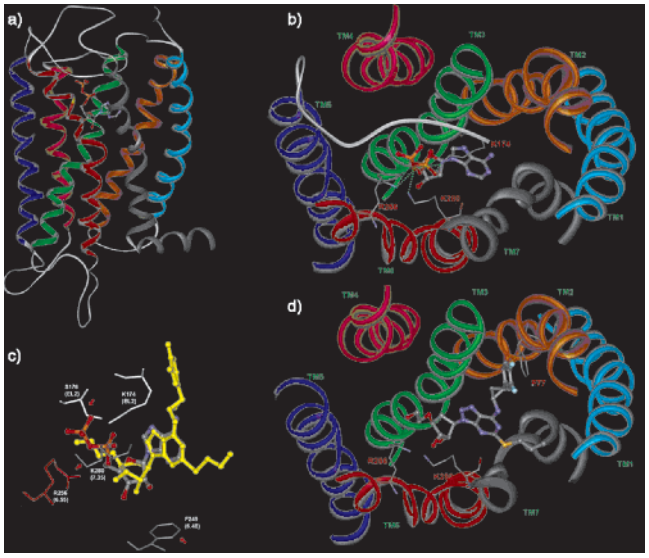


**Figure 6.** Complexes of the $P2Y_{12}$ receptor with the agonist ADP and with the antagonist **3**. Color of TMs: cyan (TM1), orange (TM2), green (TM3), magenta (TM4), blue (TM5), red (TM6), gray (TM7). (a) View from the plane of the cell membrane of $P2Y_{12}$-ADP complex. (b) View from outside the cell of the $P2Y_1$-ADP complex. (c) Superimposition of the bound conformation of ADP and **3** (yellow). The three key cationic residues and the residues corresponding to a mutated Tyr in the $P2Y_1$ receptor are shown (indicated by red arrows). (d) View from outside the cell of $P2Y_1$/**3** complex.

the exofacial side of the same TM. Furthermore, the $P2Y_{12}$ receptor homology model with docked agonist ligand suggested that this residue, which was homologous to Y306(7.35) of the $P2Y_1$ receptor, was directly involved in the formation of the nucleotide-binding pocket.

The sequence alignment shows that these three basic residues (R6.55, K7.35, and K in EL2) were conserved among all the subtypes of the second subgroup of P2Y receptors. Experimental validation would be necessary to support these interactions suggested by the models.

After defining the putative ADP-binding pocket, we explored different docking possibilities for the nucleoside-like antagonist **3**. Among the possible binding modes, we chose the one that, after superimposing the $P2Y_{12}$−ADP complex on the $P2Y_{12}$−**3** complex, showed the best steric and electronic overlap between the two ligands. In the resulting model the 3,4-difluorophenyl ring of the $N^6$ substituent of **3** formed an aromatic interaction with F77(2.48). This residue was unique to $P2Y_{12}$ and could be one of the reasons for the high $P2Y_{12}$ selectivity of this antagonist.

A crystallographic determination of the human $P2Y_1$ and $P2Y_{12}$ receptor structures would be a better starting point to determine the binding mode of ligands and to study their interactions with the receptors. However, no such experimentally elucidated structure is available. Even though a rhodopsin-based homology model of a Family 1 GPCR is not as precise as a crystal structure of the receptor would be, at present it provides the closest model available, especially if, as in this study, it comes from a careful sequence analysis. The implications of the high-resolution structure of bovine rhodopsin[5a] for structure−function analysis of Family 1 GPCRs has been well described and justified by Ballesteros and co-workers in a recent review.[35]

Our docking studies took into account the available pharmacological and mutagenesis data to distinguish multiple modes of docking of a given agonist or antagonist ligand. The selection of a given preferred docking mode was consistent with the available biological data, rather than being based on computational results alone. In fact, the binding modes selected were the only ones that were compatible with the biological data. Furthermore, during the automatic docking procedure the binding site was always treated as flexible. In this way we allowed the amino acids in the binding site to find their interactions with the ligand even if their conformation before the docking was not determined with high precision. Using this approach to study the interaction of GPCRs with their agonists is subject to greater uncertainty than with antagonists, because the template on which the homology models are based consists of the inactive state of rhodopsin. For this reason, in the present work, in which both agonists and antagonists are docked in the human $P2Y_1$ and $P2Y_{12}$ receptor model, we describe in greater detail the binding site for the antagonists at the $P2Y_1$ receptor than the other receptor−ligand complexes.

**Orphan Receptors.** The phylogenetic tree showed a number of orphan receptors present in the same branch to which P2Y receptors belong. Therefore, it is reasonable to expect that some of these receptors belong to one of the two subgroups of P2Y receptors.[3]

A basic residue at position 6.55 (Lys in $P2Y_1$ and Arg in all other cases) was typical of all different $P2Y_1$ receptors and seemed to be essential for coordination of phosphates in both subgroups.[7,23,34] Also, the presence of a His residue at position 6.52, crucial for the activation of the $P2Y_1$ receptor by nucleotide agonists,[7,23,33] was conserved among all P2Y receptor subtypes. A hypothetical explanation of the role played by residues at 6.52 and 6.55 positions in the P2Y receptors is given in the Docking section.

This HXXR(K) motif in TM6 was characteristic of P2Y receptors but not unique; it is also seen in other receptors, such as two subtypes of cysteinyl leukotriene receptors and an apelin receptor.

We selected all the orphan receptors showing the HXXR(K) motif in TM6 and analyzed their amino acid sequences in search of the basic amino acids that were implicated in the coordination of phosphates in either P2Y subgroup. As a result of this analysis (Table 4), we found that GPR91 and GPR99 showed the presence of the three amino acids typical of the subgroup of P2Y receptors to which $P2Y_1$ belongs: R3.29, R(K)6.55, and R7.39. Thus, as suggested by our phylogenetic analysis, these two receptors were likely candidates to belong to the first subgroup of P2Y receptors. The orphan receptors H963 and GPR87 were the closest to the second subgroup of P2Y receptors. Both receptors showed the presence of two of the three residues that might be important for the phosphate coordination in the second subgroup: R6.55 and K7.35. Neither sequence, however, showed the presence of the Lys in EL2 characteristic of $P2Y_{12}$, $P2Y_{13}$, and $P2Y_{14}$. As discussed above, GPR91 and GPR87 lacked the putative disulfide bridge connecting the NT with EL3, which was present in all the known subtypes of P2Y receptors. The other receptors—GPR17, GPR34, GPR31, GPR81, and HM74—did not seem to belong to either of the two subgroups of P2Y receptors.

**Table 4.** Key Cationic Residues of P2Y Receptors and Corresponding Residues in the Orphan Receptors that Show the HXXR(K) Motif in TM6. GPR91 and GPR99 Show the Presence of the Three Amino Acids Typical of First Subgroup of P2Y Receptors (i.e., R3.29, R(K)6.55, and R7.39), while H963 and GPR87 Show the Presence of Two of the Three Residues Typical of the Second Subgroup (i.e., R6.55 and K7.35)

| | 3.29 | EL2 | 6.55 | 7.35 | 7.39 |
|---|---|---|---|---|---|
| $P2Y_1$ | R | T | K | Y | R |
| $P2Y_2$ | R | T | R | Y | R |
| $P2Y_4$ | R | L | R | Y | R |
| $P2Y_6$ | R | V | K | Y | R |
| $P2Y_{11}$ | R | N | R | Y | R |
| $P2Y_{12}$ | S | K | R | K | L |
| $P2Y_{13}$ | S | K | R | K | L |
| $P2Y_{14}$ | A | K | R | K | L |
| GPR91 | R | T | R | Y | R |
| GPR99 | R | A | R | Y | R |
| GPR87 | S | D | R | K | L |
| H963 | A | G | R | K | L |
| GPR17 | G | V | R | N | S |
| GPR31 | R | R | R | S | G |
| GPR34 | G | M | R | N | L |
| GPR81 | L | S | R | L | L |
| HM74 | L | V | R | F | L |

GPR99 (also designated GPR80) is the orphan receptor that shows the highest similarity with the known P2Y receptors, in particular with the $G_q$-coupled subtypes. However, sequence comparison revealed significant dissimilarities in the amino acids of TM7 that concur in the formation of the nucleotide binding site (i.e. residues at 7.36 and 7.43 position). In a very recent paper, He et al.,[50] demonstrated that GPR91 and GPR99 can be activated by dicarboxylic acids intermediates of the citric acid cycle. Thus, in good agreement with our model, GPR91 and GPR99 are coupled to $G_q$ and require the presence of basic amino acids at 3.29, 6.55, and 7.39 to function, although they do not belong to the $P2Y_1$ subgroup.

## Conclusions

Our sequence analysis indicates that P2Y receptors fall into two phylogenetically distinct subgroups: the first encompassing the $G_q$-coupled receptors ($P2Y_1$, $P2Y_2$, $P2Y_4$, $P2Y_6$, and $P2Y_{11}$) and the second comprising the $G_i$-coupled receptors ($P2Y_{12}$, $P2Y_{13}$, and $P2Y_{14}$).

Mutagenesis experiments driven by sequence analysis probed the role of three Tyr residues located in the putative nucleotide-binding pocket of the $P2Y_1$ receptor. Consistent with modeling results, the hydroxyl groups (possibly capable of inter- or intramolecular H-bonding) of the three Tyr residues did not play a crucial role in the ligand recognition. However, the hydroxyl groups at the side chains of Tyr203 or -306 modulated ligand affinity. Mutation of Y6.48 to Ala led to a functionally inactive receptor incapable of being stimulated by agonists; this was consistent with reports on other GPCRs.

After the construction of rhodopsin-based complete homology models of all the subtypes of P2Y receptors, we performed mutagenesis-driven automatic docking experiments at $P2Y_1$ and $P2Y_{12}$ receptors. As a result of these studies, we proposed the existence of two different sets of three basic amino acids involved in the

phosphate coordination for the two subgroups. In the case of the $P2Y_1$ subgroup, these three characteristic basic residues were R3.29, K/R6.55, and R7.39.[7,23] Among these residues, only R6.55 was common to both subgroups. In the $P2Y_{12}$ subgroup, the role of R3.29 in TM3 seemed to be fulfilled by a Lys residue in EL2, and the R7.39 in TM7 seemed to be substituted by K7.35, which was located in the same TM, but at a distance of four residues, i.e., one helical turn above. Additional mutagenesis experiments would be helpful in validating these hypotheses. Y6.48 was not directly involved in the formation of the binding pocket for either agonist or antagonist. We proposed that the importance of Y6.48 could be in transmitting a rotation induced by the binding of the agonist in the upper part of TM6 to the lower part of the helix by means of interactions with conserved aromatic amino acids present above and below position 6.48: i.e., F269(6.44), F276(6.51), and H277(6.52) in the $P2Y_1$ receptor. Consistently, H277 was found to be critical for the activation induced by nucleotide agonists but not for the recognition of nucleotide or nonnucleotide antagonists.[7,23, 33]

We selected homology models, having minimal deviation from the structure of the rhodopsin template, as starting structures for our docking studies. We thus avoided introducing theoretical assumptions with potential to drive the models far from the actual structures. Those models, especially if used in conjunction with our multiple-sequence alignment, constituted a powerful tool to generate hypotheses on the similarities and differences among the various subtypes of P2Y receptors that form the basis of the ligand selectivity. Most of the P2Y receptor models constructed in this study will have to be tested experimentally, because only two subtypes (one from each subgroup of P2Y receptors) were subjected to mutagenesis and/or ligand docking in the present study.

## Experimental Section

**Materials.** The agonist 2-MeSADP **4** and the antagonist MRS2179 **2** ($N^6$-methyl-2′-deoxyadenosine-3′,5′-bisphosphate) were from Sigma (St. Louis, MO). *myo*-[$^3$H]inositol (15 Ci/mmol) was obtained from American Radiolabeled Chemicals (St. Louis, MO). [$^3$H]MRS2279 **1** (2-chloro-$N^6$-methyl-(N)-methanocarba-2′-deoxyadenosine-3′,5′-bisphosphate) was prepared as described.[36] All oligonucleotides were synthesized by Bioserve Biotechnologies (Laurel, MD).

**Plasmid Construction and Site-Directed Mutagenesis.** The coding region of pCDNA3P2Y1 was subcloned into the pCD-PS expression vector,[23] yielding pCDP2Y1. All mutations were introduced into pCDP2Y1 with the QuikChangeTM Site-directed Mutagenesis Kit (Stratagene, La Jolla, CA). Mutations were confirmed by DNA sequencing.

**Transient Expression of Mutant Receptors in COS-7 Cells.** COS-7 cells ($2 \times 10^6$) were seeded onto 100-mm culture dishes containing 10 mL of DMEM supplemented with 10% FBS. Cells were transfected ~24 h later with plasmid DNA (10 $\mu$g of DNA/dish) according to the DEAE-dextran method and grown for an additional 48 h at 37 °C.

**Inositol Phosphate Determination.** The assay was carried out as previously described.[23] About 24 h after transfection, the cells were harvested by trypsinization and grown in six-well plates (~$10^6$ cells/well; Costar, Cambridge, MA) in DMEM culture medium supplemented with 2 $\mu$Ci of *myo*-[$^3$H]-inositol/mL. After a 24-h labeling period, cells were preincubated with 10 mM LiCl for 20 min at room temperature. The mixtures were swirled to ensure uniformity. Following the addition of the agonist 2-MeSADP, the cells were incubated for 30 min at 37 °C with 5% $CO_2$. The supernatants were removed by aspiration, and 750 $\mu$L of cold 20 mM formic acid was added to each well. Cell extracts were collected after a 30-min incubation at 4 °C and neutralized with 250 $\mu$L of 60 mM $NH_4OH$. The inositol monophosphate fraction was then isolated by anion-exchange chromatography. The content of each well was applied to a small anion-exchange column (AG-1-X8; BioRad, Hercules, CA) that had been pretreated with 15 mL of 0.1 M formic acid/3 M ammonium formate, followed by 15 mL of water. The columns were then washed with 15 mL of a solution containing 5 mM sodium borate and 60 mM sodium formate. [$^3$H]Inositol phosphates (IPs) were eluted twice with 5 mL of 0.1 M formic acid/0.2 M ammonium formate, and radioactivity was quantified by liquid scintillation counting (LKB Wallace 1215 Rackbeta scintillation counter).

**Radioligand Binding Assays.** $P2Y_1$ receptor binding experiments were performed as previously described.[36] Briefly, the binding of [$^3$H]**1** (8.0 nM) to recombinant human $P2Y_1$ receptors in COS cell membranes (40 $\mu$g protein/tube) was measured after incubation at 4 °C for 30 min in 200 $\mu$L of 50 mM Tris·HCl (pH 7.4) containing 10 mM $MgCl_2$. Binding reactions were terminated by filtration through Whatman GF/B glass-fiber filters under reduced pressure with a MT-24 cell harvester (Brandel, Gaithersburg, MD), and radioactivity was determined with a liquid scintillation counter (Parkard, IL).

**Statistical Analysis.** Binding and functional parameters were calculated with Prism software (GraphPAD, San Diego, CA). $IC_{50}$ values were obtained from competition curves. Data were expressed as mean ± standard error.

**Sequence Retrieval.** The amino acid sequences of the P2Y receptors and the other GPCRs showing high similarity with them were retrieved by a BLAST search against the *H. sapiens* subset of the SWISS−PROT and TrEMBL databases (performed with the BLASTP program, local at the ExPASy server www.expasy.org/tools/blast/) using the sequences of $P2Y_1$ and $P2Y_{12}$ receptors as probes.

**Multiple-Sequence Alignment.** The seven TMs were identified and manually aligned by means of the characteristic *conservation pattern* defined by van Rhee and Jacobson.[11,37] The length of each of the seven TMs was deduced by analyzing the crystal structure of bovine rhodopsin with no gaps allowed within the TMs. The remaining parts of the sequences (the amino-terminal region, the loops, and the carboxyl-terminal region) were aligned automatically with the program CLUSTALX,[12] the Windows interface of CLUSTALW.[13] The BLOSUM62 substitution matrix[38] was used, with a gap start penalty of 5 and a gap extend penalty of 0.2. The obtained alignment was then manually refined, without allowing the TM regions to move, iteratively with the homology modeling results. Because of the lack of sequence similarity, only short segments of the amino-terminal domain and of the carboxyl-terminal domain were aligned.

**Residue Indexing.** The convention used for the amino acid identifiers, according to the approach of Ballesteros and Weinstein[10] and van Rhee and Jacobson,[11] facilitates comparison of aligned residues within the family of Group A GPCRs. The most conserved residue in a given TM (TMX, where X is the TM number) is assigned the number X.50, and residues within a given TM are then indexed relative to the 50 position. When we refer to a particular receptor, the residues maintain their original sequence number and are supplemented with the extension containing the residue identifier in brackets. When we refer to multiple receptors, the residues are designated only with the amino acid identifier.

**Phylogenetic Analysis.** A pairwise distance matrix was calculated with the Protdist program of the Phylip Package[39] with the Dayhoff PAM substitution matrix.[15] The calculated distances were scaled in units of the expected fraction of amino acids changed. From the pairwise distance matrix, the phylogenetic tree was calculated according to the Neighbor-Joining method of Saitou and Nei,[14] as implemented in the program Neighbor (Phylip Package). The resulting phylogenetic tree was constructed and plotted with the program PhyloDraw.[40]

Bootstrapping of the sequences and consensus analysis were carried out with the Seqboot and Consense programs (Phylip Package), respectively.

**Secondary Structure Prediction.** The secondary structure of the carboxyl-terminal region of the receptors was predicted by means of a Multivariate Linear Regression Combination (MLRC)[41] performed on the results obtained using the GOR4,[42] SIMPA96,[43] and SOPMA[44] methods, as implemented in the program Network Protein Sequence Analysis web server (http://npsa-pbil.ibcp.fr).[45]

**Homology Modeling.** Homology modeling was performed with the program Modeler[26,27] as implemented in InsightII,[46] with the X-ray crystal structure of bovine rhodopsin[5] (1F88.pdb, freely available at the RCSB Protein Data Bank) with a 2.8-Å resolution as a structural template. For each receptor, five models with different conformations of the loops were built (setting the input parameters of Modeler to one model and five loop refinements, with the level of optimization set to high and the manual-definition disulfide bridges assumed to exist in the extracellular region by homology to the $P2Y_1$ receptor.[6]) Because of the lack of sequence similarity between the P2Y receptors and the template in the carboxyl-terminal and carboxyl-terminal regions, only short segments of these domains were modeled. In particular, all the models started with the amino acid located three residues before the conserved Cys in the amino-terminal region of P2Y receptors and finished with the amino acid corresponding to the end of H8 in the carboxyl-terminal region of rhodopsin. According to our secondary-structure predictions, shorter H8 regions were modeled for $P2Y_4$, $P2Y_{12}$, and $P2Y_{13}$, and for $P2Y_2$ and $P2Y_{11}$, the models were terminated at the level of the last amino acid of TM7. The crude models coming from Modeler were capped with an acetyl group at the amino-terminus and with an *N*-methyl group at the carboxyl-terminus to prevent electrostatic interactions and were optimized by means of the Discover3 module of InsightII,[46] with the AMBER[47] force field. A harmonic restraint of 25 kcal/mol was applied to the backbone atoms of the TMs and EL2. The structures were minimized until an RMS of 0.5 kcal $mol^{-1}$ $Å^{-1}$ was reached; an NVT (constant-volume/constant-temperature) molecular dynamic simulation of 50 ps at 300 K was carried out, with a time step of 1 fs; the average structures from the last 10-ps trajectory of MD were reminimized until an RMS of 0.5 kcal $mol^{-1}$ $Å^{-1}$ was reached. The harmonic restraints were gradually lowered in steps of 5 kcal/mol, minimizing the structure at each step until an RMS of 0.5 kcal $mol^{-1}$ $Å^{-1}$ was reached. When the restraints were finally removed, the structures were submitted to the final energy minimization until an RMS of 0.001 kcal $mol^{-1}$ $Å^{-1}$ was reached.

**Docking Studies.** After prepositioning the ligand in the receptor cavity according to the mutagenesis and previous modeling results[6,7,8,9,23] in the case of $P2Y_1$ and by analogy in the case of $P2Y_{12}$, automatic docking experiments were carried out by means of the Monte Carlo minimization approach implemented in the Affinity module of InsightII.[46] First, an initial docking procedure, aimed at exploring different binding possibilities, was performed with the scaling factor for van der Waals and Coulombic terms set at 0.1 and 0.0, respectively, and the maximum movement in each random translation and rotation of the ligand at 1.0 Å and 10°, respectively. The preferred binding mode was chosen on the basis of compatibility with mutagenesis and binding data, as well as energetic considerations. Then, a second docking procedure, aimed at refining the binding mode resulting from the previous step, was performed, setting the scaling factor for van der Waals and Coulombic terms at 1 and the maximum movement in each random translation and rotation of the ligand at 0.1 Å and 1°, respectively. The Consistent Force Field[48,49] (CFF91) was selected for this study. This force field can describe several different chemical situations, being parametrized for a high number of atom types, and is particularly good for treating nonbonded interactions, which are of extreme importance in the study of intermolecular interactions.

**Acknowledgment.** We thank Profs. T. K. Harden and R. Nicholas of the Department of Pharmacology of the University of North Carolina, Chapel Hill, for helpful discussions, and Heng T. Duong (NIDDK) for suggestions on the manuscript.

**Supporting Information Available:** Sequence alignment, in Clustal[12,13] format, of human P2Y receptors, 60 other human G protein-coupled receptors showing high similarity with them, and the template bovine rhodopsin; 3D coordinates of optimized homology models of human $P2Y_1$, $P2Y_2$, $P2Y_4$, $P2Y_6$, $P2Y_{11}$, $P2Y_{12}$, $P2Y_{13}$, and $P2Y_{14}$ receptors in PDB format; RMS deviation between the backbone atoms of the 7TMs of human P2Y receptor models and crystal structure of bovine rhodopsin. This material is available free of charge via the Internet at http://pubs.acs.org.

## References

(1) Jacobson, K. A.; Jarvis, M. F.; Williams, M. Purine and Pyrimidine (P2) Receptors as Drug Targets. *J. Med. Chem.* **2002**, *45*, 4057−4093.

(2) Chambers, J. K.; Macdonald, L. E.; Sarau, H. M.; Ames, R. S.; Freeman, K.; Foley, J. J.; Zhu, Y.; McLaughlin, M. M.; Murdock, P.; McMillan, L.; Trill, J.; Swift, A.; Aiyar, N.; Taylor, P.; Vawter, L.; Naheed, S.; Szekeres, P.; Hervieu, G.; Scott, C.; Watson, J. M.; Murphy, A. J.; Duzic, E.; Klein, C.; Bergsma, D. J.; Wilson, S.; Livi, G. P. A G Protein-Coupled Receptor for UDP-Glucose. *J. Biol. Chem.* **2000**, *275*, 10767−10771.

(3) Abbracchio, M. P.; Boeynaems, J. M.; Barnard, E. A.; Boyer, J. L.; Kennedy, C.; Miras-Portugal, M. T.; King, B. F.; Gachet, C.; Jacobson, K. A.; Weisman, G. A.; Burnstock, G. Characterization of the UDP-Glucose Receptor (Re-named Here the $P2Y_{14}$ Receptor) Adds Diversity to the P2Y Receptor Family. *Trends Pharmacol. Sci.* **2003**, *24*, 52−55.

(4) White, P. J.; Webb, T. E.; Boarder, M. R. Characterization of a $Ca^{2+}$ Response to Both UTP and ATP at Human $P2Y_{11}$ Receptors: Evidence for Agonist-Specific Signaling. *Mol. Pharmacol.* **2003**, *63*, 1356−1363.

(5) Palczewski, K.; Kumasaka, T.; Hori, T.; Behnke, C. A.; Motoshima, H.; Fox, B. A.; Le Trong, I.; Teller, D. C.; Okada, T.; Stenkamp, R. E.; Yamamoto, M.; Miyano, M. Crystal Structure of Rhodopsin: A G Protein-Coupled Receptor. *Science.* **2000**, *289*, 739−745. (b) Teller, D. C.; Okada, T.; Behnke, C. A.; Palczewski, K.; Stenkamp, R. E. Advances in Determination of a High-Resolution Three-Dimensional Structure of Rhodopsin, a Model of G-Protein-Coupled Receptors (GPCRs). *Biochemistry* **2001**, *40*, 7761−7772. (c) Okada, T.; Fujiyoshi, Y.; Silow, M.; Navarro, J.; Landau, E. M.; Shichida, Y. Functional Role of Internal Water Molecules in Rhodopsin Revealed by X-ray Crystallography. *Proc. Natl. Acad. Sci. U.S.A.* **2002**, *99*, 5982−5987. (d) Yeagle, P. L.; Choi, G.; Albert, A. D. Studies on the Structure of the G Protein-Coupled Receptor Rhodopsin Including the Putative G-Protein Binding Site in Unactivated and Activated Forms. *Biochemistry* **2001**, *40*, 11932−11937.

(6) Hoffmann, C.; Moro, S.; Nicholas, R. A.; Harden, T. K.; Jacobson, K. A. The Role of Amino Acids in Extracellular Loops of the Human $P2Y_1$ Receptor in Surface Expression and Activation Processes. *J. Biol. Chem.* **1999**, *274*, 14639−14647.

(7) Moro, S.; Guo, D.; Camaioni, E.; Boyer, J. L.; Harden, T. K.; Jacobson, K. A. Human $P2Y_1$ Receptor: Molecular Modeling and Site-Directed Mutagenesis as Tools to Identify Agonist and Antagonist Recognition Sites. *J. Med. Chem.* **1998**, *41*, 1456−1466.

(8) Moro, S.; Hoffmann, C.; Jacobson, K. A. Role of the Extracellular Loops of G Protein-Coupled Receptors in Ligand Recognition: A Molecular Modeling Study of the Human $P2Y_1$ Receptor. *Biochemistry.* **1999**, *38*, 3498−3507.

(9) Kim, H. S.; Barak, D.; Harden, T. K.; Boyer, J. L.; Jacobson, K. A. Acyclic and Cyclopropyl Analogues of Adenosine Bisphosphate Antagonists of the $P2Y_1$ Receptor: Structure−Activity Relationships and Receptor Docking. *J. Med. Chem.* **2001**, *44*, 3092−3108.

(10) Ballesteros, J. A.; Weinstein, H. Integrated Methods for the Construction of Three-Dimensional Models and Computational Probing of Structure−Function Relations in G-Protein Coupled Receptors. *Methods Neurosci.* **1995**, *25*, 366−428.

(11) van Rhee, A. M.; Jacobson, K. A. Molecular Architecture of G Protein-Coupled Receptors. *Drug Dev. Res.* **1996**, *37*, 1−38.

(12) Thompson, J. D.; Gibson, T. J.; Plewniak, F.; Jeanmougin, F.; Higgins, D. G. The CLUSTAL_X Windows Interface: Flexible Strategies for Multiple Sequence Alignment Aided by Quality Analysis Tools. *Nucleic Acids Res.* **1997**, *25*, 4876−4882.

(13) Thompson, J. D.; Higgins, D. G.; Gibson, T. J. CLUSTAL W: Improving the Sensitivity of Progressive Multiple Sequence Alignment Through Sequence Weighting, Position-Specific Gap Penalties and Weight Matrix Choice. *Nucleic Acids Res.* **1994**, *22*, 4673−4680.
(14) Saitou, N.; Nei, M. The Neighbor-Joining Method: A New Method for Reconstructing Phylogenetic Trees. *Mol Biol Evol.* **1987**, *4*, 406−425.
(15) Dayhoff, M. O. *Atlas of Protein Sequence and Structure*; National Biomedical Research Foundation: Washington, DC, 1978; vol. 5, suppl. 3, pp 345−352.
(16) Xu, Y. Sphingosylphosphorylcholine and Lysophosphatidylcholine: G Protein-Coupled Receptors and Receptor-Mediated Signal Transduction. *Biochim. Biophys. Acta* **2002**, *1582*, 81−88.
(17) Noguchi, K.; Ishi, S.; Shimizu, T. Identification of P2y9/GPR23 as Novel G Protein-Coupled Receptor for Lysophosphatidic Acid, Structurally Distant from the Edg Family. *J. Biol. Chem.* **2003**, *278*, 25600−25606.
(18) Coughlin, S. R. How the Protease Thrombin Talks to Cells. *Proc. Natl. Acad. Sci. U.S.A.* **1999**, *96*, 11023−11027.
(19) Wise, A.; Foord, S. M.; Fraser, N. J.; Barnes, A. A.; Elshourbagy, N.; Eilert, M.; Ignar, D. M.; Murdock, P. R.; Steplewski, K.; Green, A.; Brown, A. J.; Dowell, S. J.; Szekeres, P. G.; Hassall, D. G.; Marshall, F. H.; Wilson, S.; Pike, N. B. Molecular Identification of High and Low Affinity Receptors for Nicotinic Acid. *J. Biol. Chem.* **2003**, *278*, 9869−9874.
(20) Fredriksson, R.; Lagerstrom, M. C.; Lundin, L. G.; Schioth, H. B. The G-Protein-Coupled Receptors in the Human Genome Form Five Main Families. Phylogenetic Analysis, Paralogon Groups, and Fingerprints. *Mol. Pharmacol.* **2003**, *63*, 1256−1272.
(21) Vassilatis, D. K.; Hohmann, J. G.; Zeng, H.; Li F.; Ranchalis, J. E.; Mortrud, M. T.; Brown, A.; Rodriguez, S. S.; Weller, J. R.; Wright, A. C.; Bergmann, J. E.; Gaitanaris, G. A. The G Protein-Coupled Receptor Repertoires of Human and Mouse. *Proc. Natl. Acad. Sci. U.S.A.* **2003**, *100*, 4903−4908.
(22) Fritze, O.; Filipek, S.; Kuksa, V.; Palczewski, K.; Hofmann, K. P.; Ernst, O. P. Role of the conserved NPxxY(x)5, 6F motif in the rhodopsin ground state and during activation. *Proc. Natl. Acad. Sci. U.S.A.* **2003**, *100*, 2290−2295.
(23) Jiang, Q.; Guo, D.; Lee, B. X.; van Rhee, A. M.; Kim, Y. C.; Nicholas, R. A.; Schachter, J. B.; Harden, T. K.; Jacobson, K. A. A mutational analysis of residues essential for ligand recognition at the human $P2Y_1$ receptor. *Mol. Pharmacol.* **1997**, *52*, 499−507.
(24) Costanzi, S.; Lambertucci, C.; Vittori, S.; Volpini, R.; Cristalli, G. 2- and 8-Alkynyladenosines: Conformational Studies and Docking to Human Adenosine $A_3$ Receptor Can Explain Their Different Biological Behavior. *J. Mol. Graph. Model.* **2003**, *21*, 253−262.
(25) Gao, Z. G.; Kim, S. K.; Biadatti, T.; Chen, W.; Lee, K.; Barak, D.; Kim, S. G.; Johnson, C. R.; Jacobson, K. A. Structural Determinants of $A_3$ Adenosine Receptor Activation: Nucleoside Ligands at the Agonist/Antagonist Boundary. *J. Med. Chem.* **2002**, *45*, 4471−4484.
(26) Sali, A.; Blundell, T. L. Comparative Protein Modelling by Satisfaction of Spatial Restraints. *J. Mol. Biol.* **1993**, *234*, 779−815.
(27) Sali, A.; Overington, J. P. Derivation of rules for comparative protein modeling from a database of protein structure alignments. *Protein Sci.* **1994**, *3*, 1582−1596.
(28) Laskowski, R. A.; MacArthur, M. W.; Moss, D. S. Thornton. J. M. PROCHECK: A Program to Check the Stereochemical Quality of Protein Structures. *J. Appl. Crystallogr.* **1993**, *26*, 283−291.
(29) Morris, A. L.; MacArthur, M. W.; Hutchinson, E. G.; Thornton, J. M. Stereochemical Quality of Protein Structure Coordinates. *Proteins* **1992**, *12*, 345−364.
(30) Heller, H.; Schaefer, M.; Schulten, K. Molecular Dynamics Simulation of a Bilayer of 200 Lipids in the Gel and in the Liquid-Crystal Phases. *J. Phys. Chem.* **1993**, *97*, 8343−8360.
(31) Nandanan, E.; Jang, S. Y.; Moro, S.; Kim, H. O.; Siddiqui, M. A.; Russ, P.; Marquez, V. E.; Busson, R.; Herdewijn, P.; Harden, T. K.; Boyer, J. L.; Jacobson, K. A. Synthesis, Biological Activity, and Molecular Modeling of Ribose-Modified Deoxyadenosine Bisphosphate Analogues as $P2Y_1$ Receptor Ligands. *J. Med. Chem.* **2000**, *43*, 829−842.
(32) Springthorpe, B. From ATP to AZD6140: Design of an Orally Active $P2Y_{12}$ ($P_{2T}$) Receptor Antagonist for the Treatment of Thrombosis. 16 MEDI, 225th ACS National Meeting, New Orleans, LA, March 23−27, 2003.
(33) Guo, D.; von Kügelgen, I.; Moro, S.; Kim, Y.-C.; Jacobson, K. A. Evidence for the Recognition of Nonnucleotide Antagonists Within the Transmembrane Domains of the Human $P2Y_1$ Receptor. *Drug Dev. Res.*, **2002**, *57*, 173−181.
(34) Cattaneo, M.; Zighetti, M. L.; Lombardi, R.; Martinez, C.; Lecchi, A.; Conley, P. B.; Ware, J.; Ruggeri, Z. M. Molecular Bases of Defective Signal Transduction in the Platelet $P2Y_{12}$ Receptor of a Patient with Congenital Bleeding. *Proc. Natl. Acad. Sci. U.S.A.* **2003**, *100*, 1978−1983.
(35) Ballesteros, J. A.; Shi, L.; Javitch, J. A. Structural Mimicry in G Protein-Coupled Receptors: Implications of the High-Resolution Structure of Rhodopsin for Structure−Function Analysis of Rhodopsin-like Receptors. *Mol. Pharmacol.* **2001**, *60*, 1−19. Review. Erratum in: *Mol. Pharmacol.* **2002**, *61*, 247.
(36) Waldo, G. L.; Corbitt, J.; Boyer, J. L.; Ravi, G.; Kim, H. S.; Ji, X. D.; Lacy, J.; Jacobson, K. A.; Harden, T. K. Quantitation of the $P2Y_1$ Receptor With a High Affinity Radiolabeled Antagonist. *Mol. Pharmacol.* **2002**, *62*, 1249−1257.
(37) van Rhee, A. M.; Fischer, B.; van Galen, P. J.; Jacobson, K. A. Modelling the P2Y Purinoceptor Using Rhodopsin as Template. *Drug Des. Discovery* **1995**, *13*, 133−154.
(38) Henikoff, S.; Henikoff, J. G. Amino Acid Substitution Matrixes from Protein Blocks. *Proc. Natl. Acad. Sci. U.S.A.* **1992**, *89*, 10915−10919.
(39) PHYLIP Phylogeny Inference Package, Version 3.6, July 2002, Joseph Felsenstein, Department of Genome Sciences, University of Washington, Seattle, WA.
(40) PhyloDraw, Version 0.8, Graphics Application Lab., Department of Computer Science, Pusan National University, Pusan, South Korea.
(41) Guermeur, Y.; Geourjon, C.; Gallinari, P.; Deleage, G. Improved Performance in Protein Secondary Structure Prediction by Inhomogeneous Score Combination. *Bioinformatics* **1999**, *15*, 413−421.
(42) Garnier, J.; Gibrat, J. F.; Robson, B. GOR Method for Predicting Protein Secondary Structure from Amino Acid Sequence. *Methods Enzymol.* **1996**, *266*, 540−553.
(43) Levin, J. M.; Robson, B.; Garnier, J. An Algorithm for Secondary Structure Determination in Proteins Based on Sequence Similarity. *FEBS Lett.* **1986**, *205*, 303−308.
(44) Geourjon, C.; Deleage, G. SOPMA: Significant Improvements in Protein Secondary Structure Prediction by Consensus Prediction from Multiple Alignments. *Comput. Appl. Biosci.* **1995**, *11*, 681−684.
(45) Combet, C.; Blanchet, C.; Geourjon, C.; Deleage G. NPS@: Network Protein Sequence Analysis. *Trends Biochem. Sci.* **2000**, *25*, 147−150.
(46) InsightII, Version 2001, Accelrys Inc.
(47) Weiner, S. J.; Kollman, P. A.; Case, D. A.; Singh, U. C.; Ghio, C.; Alagona, G.; Profeta, S. J.; Weiner, P. A New Force Field for Molecular Mechanical Simulation of Nucleic Acids and Proteins. *J. Am. Chem. Soc.* **1984**, *106*, 765−784.
(48) Maple, J. R.; Hwang, M. J.; Stockfisch, T. P.; Dinur, U.; Waldman, M.; Ewig, C. S.; Hagler, A. T. Derivation of Class II Force Fields. 1. Methodology and Quantum Force Field for the Alkyl Functional Group and Alkane Molecules. *J. Comput. Chem.* **1994**, *15*, 162−182.
(49) Hwang, M. J.; Stockfisch, T. P.; Hagler, A. T. Derivation of Class II Force Fields. 2. Derivation and Characterization of a Class II Force Field, CFF93, for the Alkyl Functional Group and Alkane Molecules. *J. Am. Chem. Soc.* **1994**, *116*, 2515−2525.
(50) He, W.; Miao, F. J. P.; Lin, C. H.; Schwandner, R. T.; Wang, Z.; Gao, J.; Chen, J. L.; Tian, H.; Ling, L. Citric acid cycle intermediates as ligands for orphan G-protein-coupled receptors. *Nature* **2004**, *429*, 188−193.
(51) Ding, Z.; Kim, S.; Dorsam, R. T.; Jin, J.; Kunapuli, S. P. Inactivation of the human $P2Y_{12}$ receptor by thiol reagents requires interaction with both extracellular cysteine residues, Cys17 and Cys270. *Blood* **2003**, *101*, 3908−3914.

JM049914C